Sebastian Matich, Markus Hessinger, Mario Kupnik, Roland Werthschützky, and Christian Hatzfeld*

Miniaturized multiaxial force/torque sensor with a rollable hexapod structure

Miniaturisierter Kraft-Momenten-Sensor auf Basis einer gerollten Hexapod-Struktur

DOI 10.1515/teme-2017-0046

Abstract: Miniaturized force/torque sensors are relevant components for robotic interaction with humans and unknown environments. This paper presents a disruptive manufacturing process for multiaxial force/torque sensors based on a Stewart-Gough platform. The deformation element consists of a hexapod geometry with six sensing elements with a total diameter of 9 mm. The sensor manufacturing process is divided into three steps: 1. Milling a planar arrangement of sensing elements out of a 2 mm steel (1.4301) plate, 2. applying twelve strain gauges in half-bridge configuration and 3. rolling the elements into a hexapod structure. The dimensions of the sensing elements are scalable to adjust the size and nominal measurement range of the sensor. The first prototype has a measuring range of 4 N and 66 mNm. The characterization of the sensor shows a maximal linearity and hysteresis error of 1.16 % and a cross-sensitivity smaller than 2.76 %.

Keywords: Force/torque sensor, disruptive design, miniaturization.

Zusammenfassung: Miniaturisierte Kraft-Momenten-Sensoren sind notwendige Komponenten für die Interaktion von Robotern mit Menschen und unbekannten Umgebungen. In dieser Arbeit wird ein neuartiger Ansatz zur Fertigung solcher Sensoren auf Basis einer Stewart-Gough-Plattform präsentiert. Der so gefertigte Sensor basiert auf einem sechseckigen Verformungskörper mit einem Durchmesser von 9 mm. Der Fabrikationsprozess besteht aus drei Schritten: 1. Fräsen einer planaren Struktur mit aus einer Stahlplatte mit einer Dicke von 2 mm, 2. Applikation von zwölf Metallfolien-DMS in einer Halbbrücken-Konfiguration und 3. Aufrollen des Verformungskörpers. Die Größe des Verformungskörpers kann dabei einfach an verschiedene Messbereiche angepasst werden. Der erste so gefertigte Prototyp weist einen Messbereich von 4 N bzw. 66 mNm auf. Der Linearitäts- und Hysteresefehler beträgt 1,16 %, das Übersprechen maximal 2,76 %.

Schlüsselwörter: Kraft-Momenten-Sensor, disruptives Design, Miniaturisierung.

Sebastian Matich, Markus Hessinger, Mario Kupnik, Roland Werthschützky, Christian Hatzfeld, Technische Universität Darmstadt, Institute of Electromechanical Design, Merckstr. 25, 65283 Darmstadt, Germany. *Corresponding author: phone: +49 6151 16-23884, e-mail: c.hatzfeld@emk.tu-darmstadt.de

1 Introduction

Whenever machines interact with an unknown environment, a precise feedback of the applied forces and torques is necessary to monitor the running process and ensure safe operations. For robotic systems, an integrated force measurement sensor at the tool center point enables force feedback control during operation tasks. Several systems, e.g. for robotic assisted minimally invasive surgery [1], require a high miniaturization level of the sensors in order to operate in a small workspace. While in this case a force/torque sensor with a diameter of less than 10 mm is needed, the smallest commercially available product is the *ATI nano17* that has a footprint of 17 mm.

Several new sensor designs as well as alternative, robot specific concepts as presented by the authors [4] were introduced to measure interaction forces. New sensor designs are based on resistive, capacitive or optical measurement principles and exhibit a diameter of 10 mm and three degrees of freedom in the majority of realizations:

- *Puangmali et al.* introduced a force sensor with integrated optical fibers to measure the intensity of light that is reflected by the sensor structure [5]. Due to the proportionality between the deformation and the intensity a payload of up to 3 N can be resolved.
- Integrating to PCB discs each having three arc electrodes on it and measuring the capacity between those, *Lee et al.* showed a sensor design with a nominal load of 0,5 N [2].
- A sensor structure with an inner and an outer ring, connected by several beams with applied silicon strain gages, capable of measuring forces of up to 5 N is shown by *Rausch* [6].

While a triaxial sensor is suitable for push-pull tasks, it fails in complex handling operations that involve gripper and, therefore, interaction torques. Even those tasks are more common, only some designs of small scale force/torque sensors exist due to sensor size restrictions.

A well-known design of a six degree of freedom force/torque sensor is the one of *Seibold et al.*, whose deformation structure is based on the kinematics of a Stewart-Gough platform [8]. Figure 1 shows the 10 mm precision milled structure, that has an upper and a lower ring which are connected through six diagonal beams with flexure hinges at each end. Bonded strain gauges measure the strain in each beam, so the load force and torque is obtained by the sensor matrix which is directly related to the inverse transpose Jacobian-Matrix of the Stewart-Gough platform. The prototype is tested with a nominal load of 2.5 N and is designed to measure interaction forces during a minimally invasive surgical procedure. Considering the same use case, *Li et al.* modified the design in [3]. Instead of placing the strain gauges to the side wall of the beam, they are now accessible on the outer walls to improve manufacturability. Nevertheless, mechanical and electrical bonding processes of the sensing elements on a three-dimensional body limits scalability, process automation and increases costs. In this paper, we present a disruptive design process to obtain scalable force/torque sensors with cost-effective and reproducible mass production capabilities.

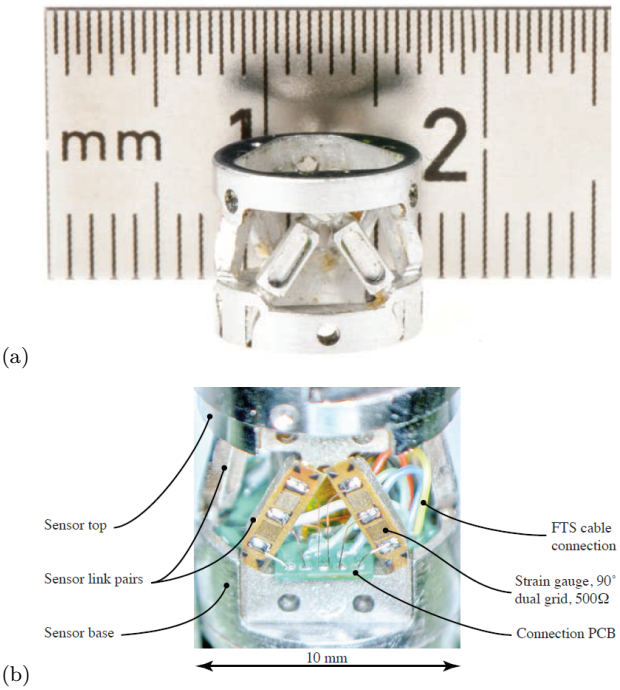

Fig. 1: Sensor designs by *Seibold et al.* (a) First monolitic prototype, (b) optimized, non-monolitic design for easier electrical connection and increased mechanical stability. Figure reproduced from [9].

2 Sensor design

The basic idea of our approach is to break with the conventional force sensor design sequence: Instead of manufacturing the entire deformation body in its final form first and applying strain sensitive elements in a second step, the deformation body is manufactured only in part first, strain gauges are applied and a final joining process yields the three dimensional sensor structure. This approach is applied to a force/torque-sensor with six degrees of freedom based on a Stewart-Gough platform.

As Figure 2 illustrates, the hexagonal kinematics can be unwound to an equivalent planar representation. This offers the opportunity to fabricate a planar deformation structure by planar process with increased precision, such as precision milling or laser cutting. In addition, electrical and mechanical bonding processes can be performed in plane, too. Afterwards, the 3D-structure is obtained by rolling the planar structure.

Figure 2c shows the design of the planar structure. It has six strain gauge application areas with spherical flexure hinges at both ends to transfer the mechanical load. Milled cavities on the backside of the strain gauge application areas locally decrease the thickness d. Thus, the nominal strain ϵ_N on the surface can be adjusted by the design parameter d to meet the requirements of the strain detecting technology. In this case, we chose $\epsilon_N = 0.5\,\mathrm{mm\,m^{-1}}$ for standard metal foil strain gauges. The deformation body is manufactured from stainless steel (type 1.4301) with a precision milling machine.

Twelve foil strain gauges (type 1-LY11-0.3/120, HBM GmbH, Germany) are applied to the planar deformation element to measure load-induced strain (Fig. 3). Two are wired in a half-bridge configuration for each flexure hinge to minimize temperature influences. The planar bonding of all strain gauges in a single process step enables a reproducible interlayer thickness to reduce hysteresis effects. Solder terminals located on the upper and lower end of each segment facilitate the electrical connection of the half-bridge circuits.

Since the segments are connected through integral hinges (Fig. 2c), the intended three-dimensional structure of the sensor is obtained by rolling the planar part (Fig. 2d) into a hexagonal structure. Two circular flanges are pinned

to the end faces to establish the mechanical link between the individual segments and to enable sensor installation. Parts are aligned by inserting them into a tube with defined inner diameter to guarantee the cylindricity of the sensor. Axial pre-stressing of the setup achieves form

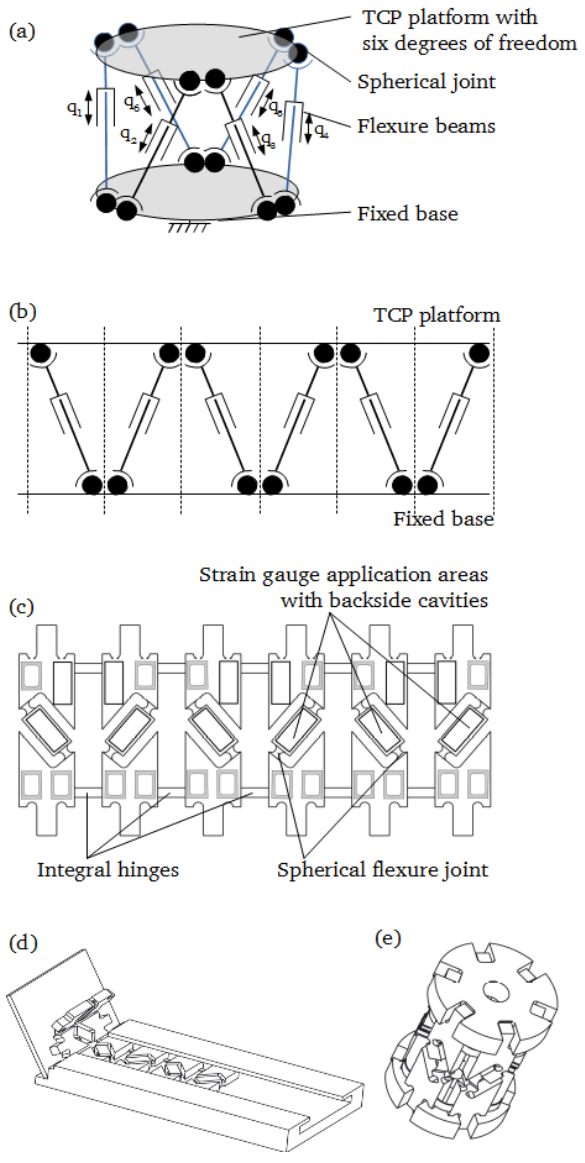

Fig. 2: Mechanical design of the sensor. (a) Steward-Gough structure, (b) unwound kinematic structure, (c) design of the deformation body, (d) rolling up the sensor, (e) complete sensor.

closure between the deformation body and the flanges (Fig. 2e). This form closure is secured with glue and finally laser welded. The final prototype exhibits a total diameter of 9 mm (Fig. 3b). The rolled-up structure also provides a basic protection against external influences, since the strain-sensitive structures are placed on the inside of it.

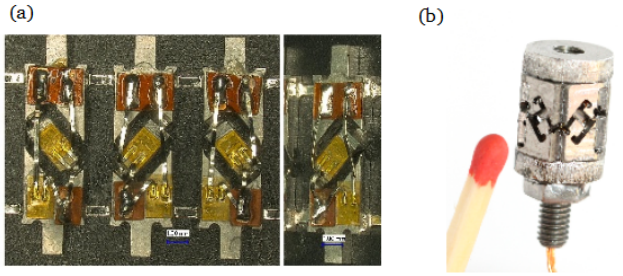

Fig. 3: Sensor fabrication. (a) Strain gauges (light brown) and solder terminals (dark brown) applied to deformation body, (b) complete sensor after rolling with strain gauges on the inside. This version does not include form closure fitting of the sensor flanges.

3 Sensor calibration

Since strains in the flexure beams of a Steward-Gough platform do not directly correspond to forces F and torques M in Cartesian space, a sensor calibration matrix is used to determine these measures from the output voltages u_i of the strain gauges:

$$\begin{pmatrix} F_x \\ F_y \\ F_z \\ M_x \\ M_y \\ M_z \end{pmatrix} = \mathbf{K} \cdot \begin{pmatrix} u_1 \\ u_2 \\ u_3 \\ u_4 \\ u_5 \\ u_6 \end{pmatrix}$$

To determine the sensor-matrix $\mathbf{K}$, known loads are applied to the sensor [7, 9]. In this case, the set-up shown in figure 4 is used. One flange of the sensor is fixed at a base plate, while a frame is fixed at the opposite sensor flange. A known load case can be generated by attaching weights with a rope guided over a diverter pulley at different points of the frame. This process is automated with a linear axis and stacked weight buckets as described in [4].

To calculate the coefficient matrix $\mathbf{K}$, six load cases described in Figure 4 are sequentially generated. Signals of the six half-bridges are recorded using six bridge terminals for an Ethercat industrial network (type EL3356-0010, Beckhoff, Verl, Germany) that are connected to a Simulink real-time target. 200 samples with a sample rate of 100 Hz are measured for each load case. The columns of the inverse transpose matrix K^{-1^t} can be calculated as the quotient of the output voltages divided by the applied load or torque value. The sensor-matrix $\mathbf{K}$ in eq. (1) is

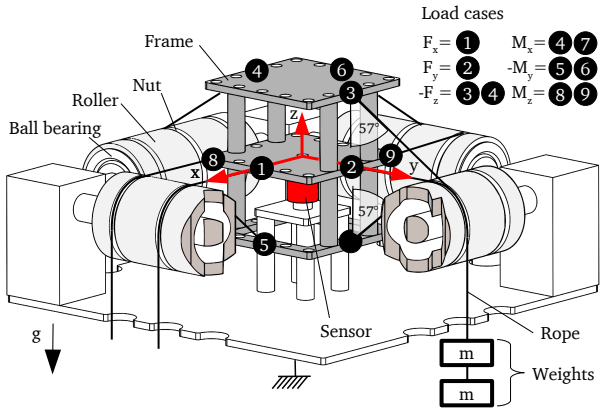

Fig. 4: Calibration set-up with mounted frame to generate the six load cases using weights attached to a rope and the shown load points.

obtained by calculating the inverse transpose.

$$\mathbf{K} = 10^{-4} \begin{pmatrix} -1.26 & -1.47 & -3.31 & -2.21 & 2.12 & 3.48 \\ -4.05 & -4.58 & -0.20 & 4.05 & -3.31 & 0.81 \\ 0.52 & 1.40 & -0.56 & 0.24 & -1.03 & 0.98 \\ 0.31 & 0.47 & -0.20 & -0.48 & 0.23 & -0.29 \\ -0.40 & 0.06 & -0.43 & -0.05 & 0.48 & 0.38 \\ -0.34 & 0.34 & 0.31 & -0.33 & -0.33 & 0.32 \end{pmatrix} \quad (1)$$

4 Results

The sensor matrix $\mathbf{K}$ is implemented on the target computer in order to investigate the sensor's characteristic. Four loading and unloading cycle up to the nominal values ($F_x = F_y = 4\,\mathrm{N}$, $F_z = 1\,\mathrm{N}$, $M_x = M_y = 60\,\mathrm{mN\,m}$, $M_z = 35\,\mathrm{mN\,m}$) are applied to the sensor. Each cycle is repeated 10 times with the automatic platform described above. For each of the 10 steps a mean value is calculated and linear characteristic curves (Fig. 5) are obtained using the least square method. Compared to this curve, the absolute error of all measurements are below 4.95 mN and 176 µN m for forces and torques, respectively (Tab. 1). This yields a linearity error of less than 0.97 % and a hysteresis error of less 1.16 %. The absolute crosstalk between channels is always smaller than 0.11 N and 0.76 mNm, respectively, i.e. a relative error of 2.76 %.

5 Conclusion and further work

The designed multiaxial force/torque sensor with a diameter of 9 mm and a measuring range of 4 N and 66 mN m demonstrates the functionality of the introduced disruptive manufacturing process. Although the sensor consists of a non-monolitic deformation body, no grave measurement errors are induced by the joining processes such as glueing and welding. The resulting errors seem to be tolerable for a variety of applications that especially depend on small and compact sensors and are in line with results from existing works (*Li et al.* report a force hysteresis error of 2.5 % in [3] but do not report linearity errors).

The planar manufacturing of the deformation element as well as the possibility to apply strain sensitive elements on a planar surface minimizes manufacturing effort and costs compared to the standard manufacturing approach by hand. Also an automated manufacturing process seems to be possible with the presented approach.

Further work will include a more detailed analysis of the measurement uncertainty of the sensor as well as exploration of model-based correction algorithms in order to minimize measurement errors. We also plan on a more detailed analysis of the unwounding step to design sensors with different sensitivities for forces and torques depending on the structure of the deformation body. Future use of smaller silicon strain gauges as developed in [6] facilitates a miniaturization level of the sensor down to 5 mm diameter.

Acknowledgment: The authors thank Walter Albrecht, Department of Electrical Engineering and Information Technology, Technische Universität Darmstadt, for helpful discussions and the manufacturing of the sensor.

References

[1] Hatzfeld, C et al. "A Teleoperated Platform for Transanal Single-Port Surgery: Ergonomics and Workspace Aspects" IEEE World Haptics Conference (WHC), 2017.

[2] Lee, DH; Kim, U & Choi, HR. "Development of multi-axial force sensing system for haptic feedback enabled minimally invasive robotic surgery." IEEE/RSJ International Conference on Intelligent Robots and Systems (IROS), 2014.

[3] Li, K et al. "A novel 4-DOF surgical instrument with modular joints and 6-Axis Force sensing capability." The International Journal of Medical Robotics and Computer Assisted Surgery 13.1 (2017).

[4] Matich, S et al. "3-D force measurement using single axis force sensors in a new single port parallel kinematics surgical manipulator." IEEE/RSJ International Conference on Intelligent Robots and Systems (IROS), 2016.

[5] Puangmali, P et al. "Optical fiber sensor for soft tissue investigation during minimally invasive surgery." IEEE International Conference on Robotics and Automation (ICRA), 2008.

[6] Rausch, J. "Entwicklung und Anwendung miniaturisierter piezoresistiver Dehnungsmesselemente" Dissertation, 2012, Technische Universität Darmstadt.

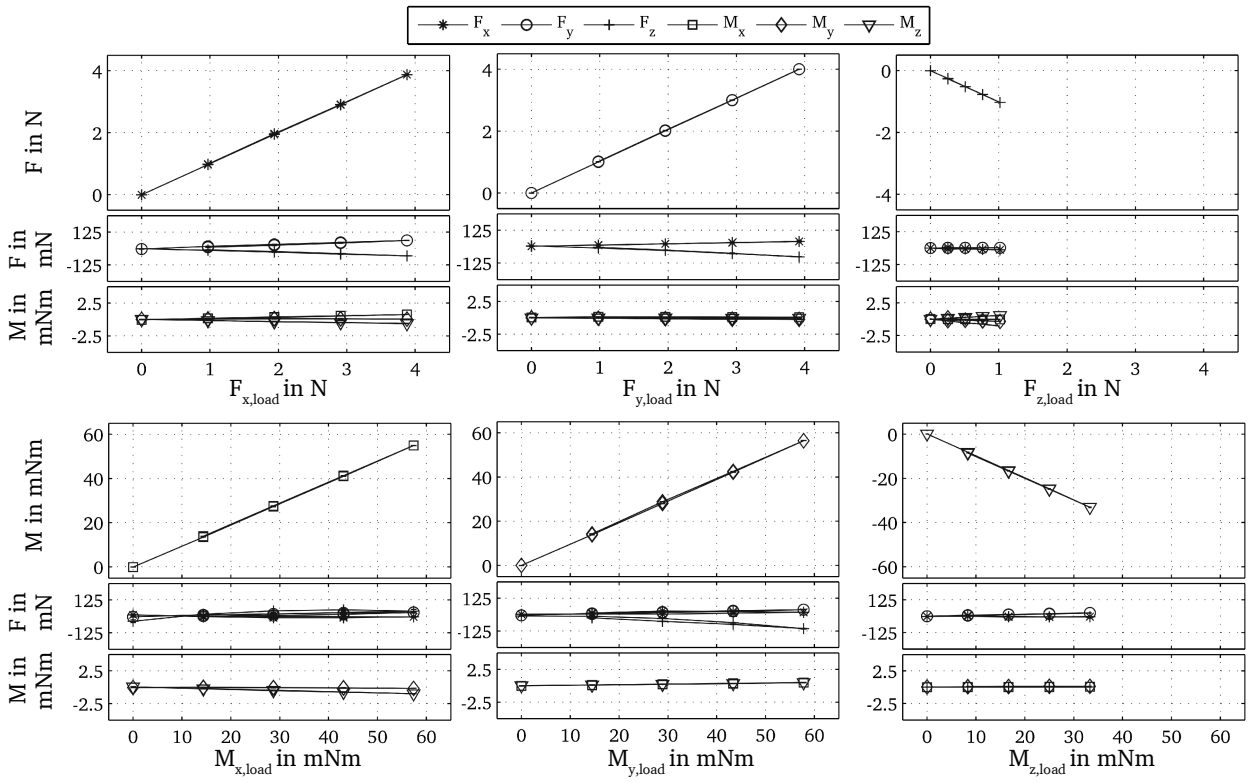

Fig. 5: Characteristic curve of the prototype.

Table 1: Characteristic of the manufactured force/torque sensor with measured linearity $k_{Channel}$, zero point error n_0, maximal scattering s_{max} and maximal linearity and hysteresis error f_{lin} and f_{Hys}. For each load case the crosstalk is given by the absolute values $q_{F,max}$ and $q_{M,max}$. Nominal loads differ slightly from specifications because of the discrete weights used for characterization.

	Nominal Load	$k_{Channel}$	n_0	s_{max}	f_{lin}	f_{Hys}	$q_{F,max}$	$q_{M,max}$
	in	**in**	**in**	**in**	**in**	**in**	**in**	**in**
Channel	**N**	**N/N**	**mN**	**mN**	**%**	**%**	**N**	**mMm**
F_x	3.88	1.00	-4.82	4.95	0.64	0.30	0.06	0.76
F_y	3.92	1.02	9.92	2.55	0.39	0.18	0.08	0.26
F_z	1.02	-1.01	-8.33	4.11	0.48	0.91	0.01	0.57
Channel	mNm	Nm/Nm	μNm	μNm	%	%	N	mNm
M_x	57.4	0.96	-61.69	71.06	0.36	0.48	0.05	0.05
M_y	57.8	0.98	36.41	63.55	0.97	0.73	0.11	0.50
M_z	-33.3	-0.99	-54.72	175.74	0.74	1.16	0.03	0.15

[7] Schleichert, J; Rahneberg, I & Fröhlich, T. "Calibration of a novel six-degree-of-freedom force/torque measurement system." International Journal of Modern Physics: Conference Series. Vol. 24, 2013.

[8] Seibold, U; Kubler, B & Hirzinger, G. "Prototype of instrument for minimally invasive surgery with 6-axis force sensing capability." IEEE International Conference on Robotics and Automation (ICRA), 2005.

[9] Seibold, U. "An Advanced Force Feedback Tool Design for Minimally Invasive Robotic Surgery", Dissertation, Technische Universität München, 2013.